Small-x physics at the Large Hadron Collider

&

at the Electron Ion Collider

Cristian Baldenegro Barrera (c.baldenegro@cern.ch)

The University of Kansas

@CrisBaldenegro

Workshop on high energy physics and related topics at Sonora, Mexico

DE-SC0019389

Outline

- High-energy limit of strong interactions and small-x limit.
- Experience from deep inelastic scattering at small-x.
- Jet probes of small-x physics at the LHC.
- Parton saturation and the future Electron Ion Collider.
- Summary.

Quarks and gluons, which carry color charge (red, green, blue) are sensitive to the strong interaction.

Two key characteristics of QCD:

- **Color confinement:** Only color-neutral particles made of quark & gluons (hadrons), are observed in isolation.
- **Asymptotic freedom:** The interaction strength decreases at short distances (high energies)

QCD is central to modern colliders

...and QCD is what we are made of

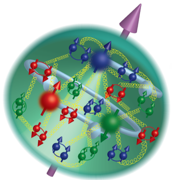

$\approx$ 98% of the mass of the proton comes from QCD binding energy.

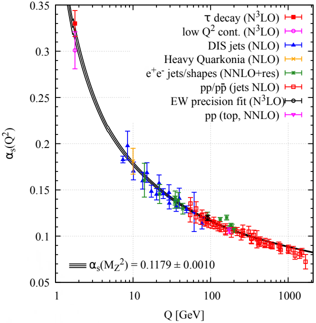

Running of the strong coupling, α_s

Plenty of open problems and questions in QCD

- How are hadrons formed starting from the fundamental degrees of freedom of QCD?
- What are the properties of the quark-gluon plasma?
- Do glueballs exist? If so, what are their properties?
- **What is the combined effect of multiple gluon splittings in high energy scattering?**
- **Does the proton/nucleus behave like a "color glass condensate" at high energies?**

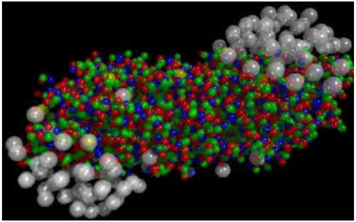

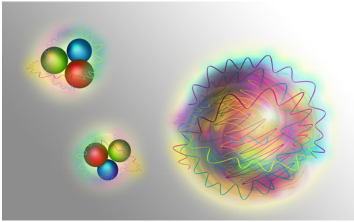

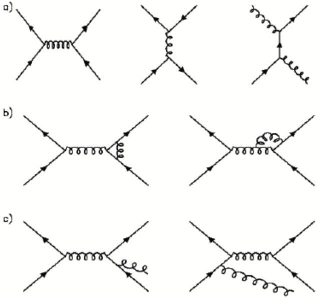

In fixed-order pQCD, we calculate the hard cross sections in powers of $\alpha_s \ll 1$, *symbolically* (ignoring pre-factors) represented by

$$\mathrm{d}\hat{\sigma} \sim \alpha_s^2 + \alpha_s^3 + \alpha_s^4 + \ldots$$

Calculations are known at leading order (LO), next-to-LO (NLO), next-to-NLO (N^2LO), and in very few cases for next-to-NNLO (N^3LO).

The high-energy limit is defined by $\hat{s} \gg -\hat{t} \gg \Lambda^2_{\text{QCD}}$, where $\hat{s}$, $\hat{t}$ are the Mandelstam variables at parton-level, **the fixed-order pQCD approach breaks down**.

The perturbative expansion should be rearranged (symbolically) as,

$$d\hat{\sigma} \simeq \alpha_s^2 \sum_{n=0}^{\infty} \alpha_s^n \ln^n\left(\frac{\hat{s}}{|\hat{t}|}\right) + \alpha_s^3 \sum_{n=0}^{\infty} \alpha_s^n \ln^n\left(\frac{\hat{s}}{|\hat{t}|}\right) + \alpha_s^4 \sum_{n=0}^{\infty} \alpha_s^n \ln^n\left(\frac{\hat{s}}{|\hat{t}|}\right) + \dots$$

such that $\alpha_s^n \ln^n(\hat{s}/|\hat{t}) \lesssim 1$.

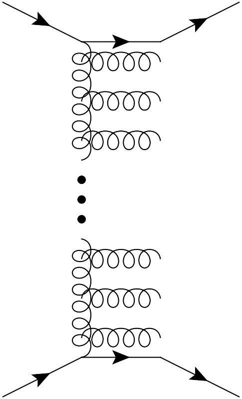

Resummation of large logarithms of $\hat{s}$ to all orders in α_s via **Balitsky-Fadin-Kuraev-Lipatov (BFKL)** evolution equations of pQCD.

Resummation known at leading logarithmic (LL) accuracy ($\alpha_s^n \ln^n(\hat{s}/|\hat{t})$ terms) and next-to-LL (NLL, $\alpha_s^{n-1} \ln^n(\hat{s}/|\hat{t})$ terms).

A notable prediction in BFKL:

$$\mathcal{M}(s,t) \propto \hat{s}^{\lambda}, \qquad \lambda^{\text{LL}} = \frac{N_c}{\pi} 4 \ln 2 \alpha_s \approx 0.25\text{–}0.5$$

Why should we care about the high energy limit of QCD anyway?

- **Important test of quantum field theory**. Relevant for QCD in particular, and for **gauge theories in general**.
- **Cosmic ray physics:** cosmic ray interactions with the atmosphere can occur at the multi-TeV scale and beyond. **The strong force dominates.**
- **Gluon saturation effects:** need to understand gluon densities in proton and heavy-ion collisions as a function of x. **An important topic of discussion at the future Electron Ion Collider.**

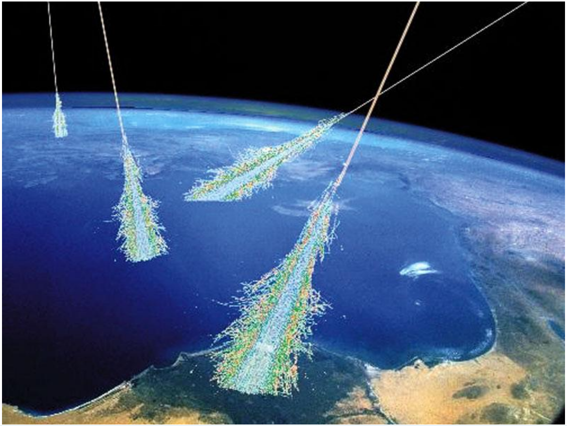

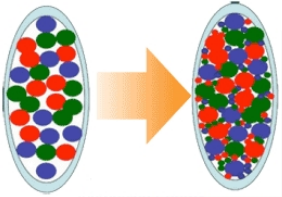

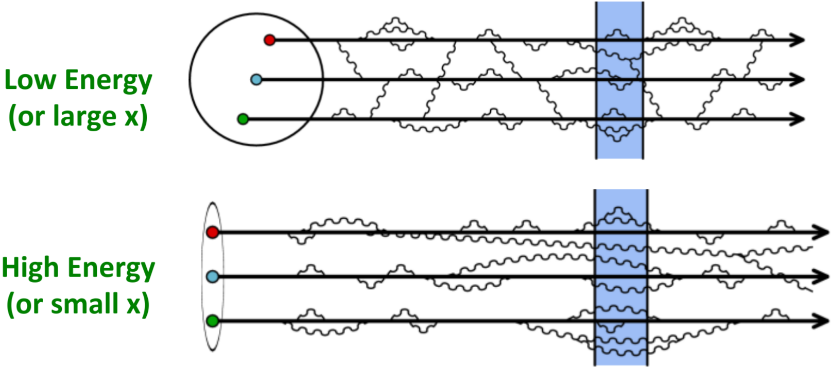

Due to universality of strong interactions, similar gluon splitting pattern emerges in the structure of the proton and nuclei at high-energies.

More and more gluons carry smaller and smaller fractions of the proton momentum x.

Small-x limit of QCD $\Longleftrightarrow$ high-energy limit of QCD scatterings.

Gluon splitting a la BFKL inside the proton

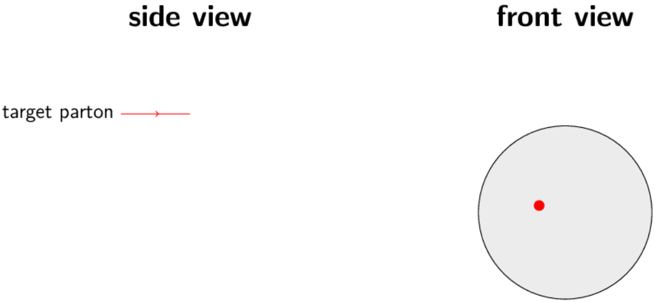

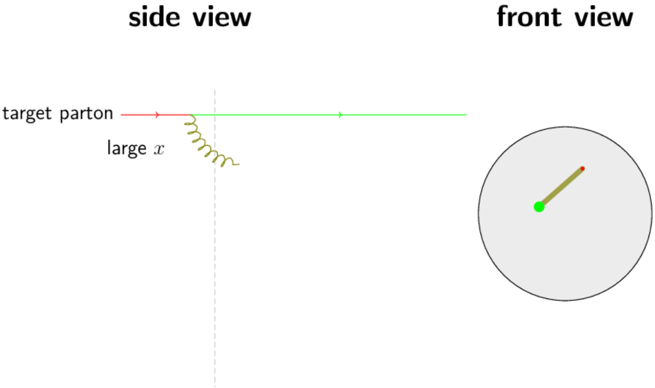
side view
front view
target parton
large x

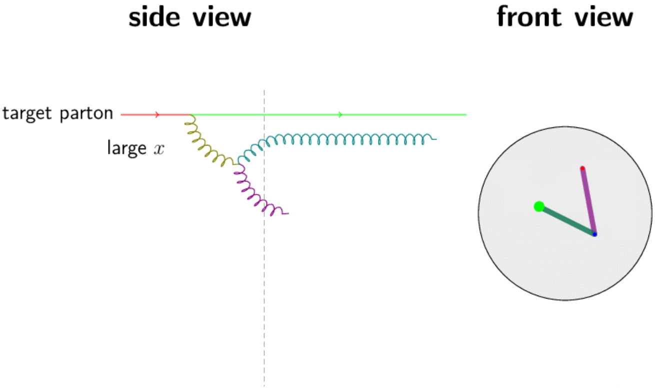
side view
front view
target parton
large x

Gluon splitting a la BFKL inside the proton

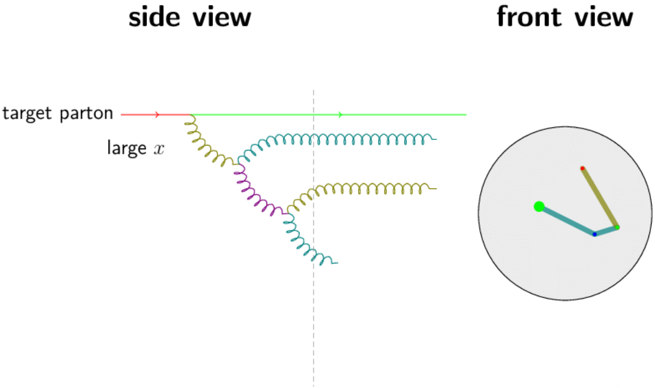

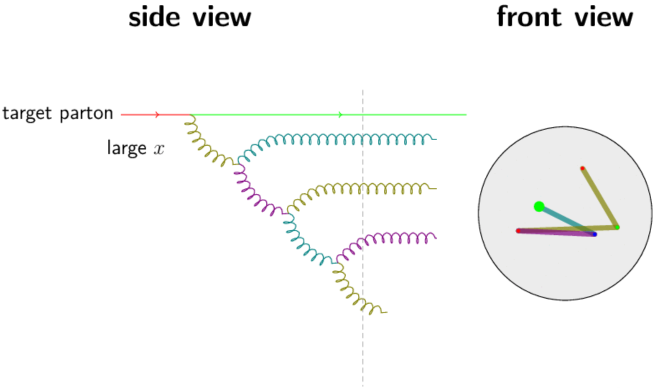
side view
front view
target parton
large x

Gluon splitting a la BFKL inside the proton

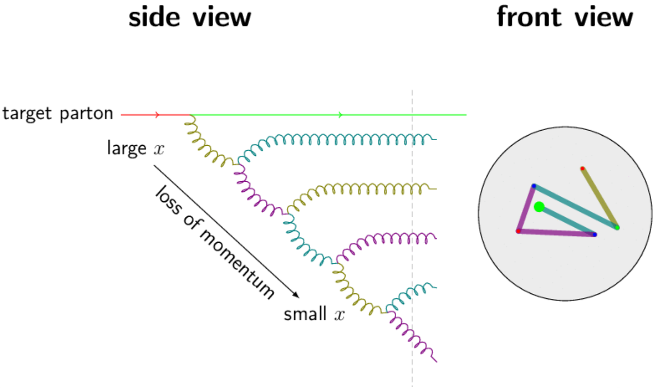

More generalized evolution of the proton wavefunction in x and Q^2

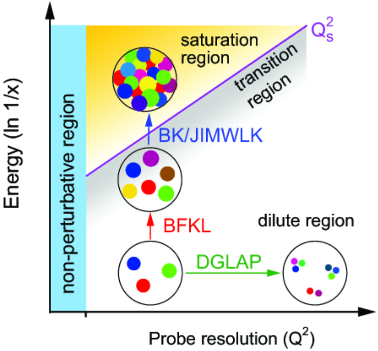

Dokshitzer-Gribov-Lipatov-Altarelli-Parisi (DGLAP): Evolution in Q^2 (resummation of $\alpha_s^n \ln^n(Q^2/Q_0^2)$) $\rightarrow$ Resolving "smaller" partons with larger Q^2.

BFKL: Evolution in x (resummation of $\alpha_s^n \ln^n(1/x)$) $\rightarrow$ Larger parton densities at smaller x at fixed Q^2.

Very important to understand parton densities QCD evolution in (x, Q^2) plane.

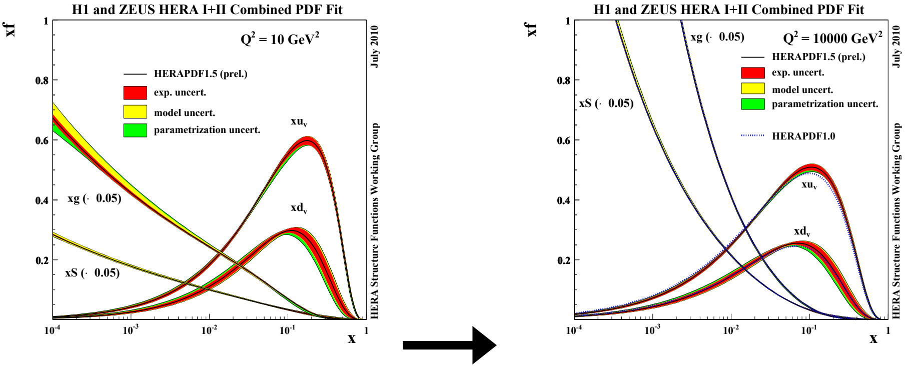

Known PDFs as a function of x at a given Q^2 $\to$ evolved to a new PDF as a function of x at a $Q^2 \to Q^2_{\text{new}}$.

PDFs used to calculate hadron-level cross sections in high-energy hadron-hadron collisions,

$$\sigma = \sum_{i,j} \int dx_1 f_i(x_1, \mu_F^2) \int dx_2 f_j(x_2, \mu_F^2) \times \hat{\sigma}(x_1, x_2, \mu_F^2, \mu_R^2) + \mathcal{O}(\Lambda^2_{QCD}/Q^2)$$

Parton densities are extracted from global fit analyses. Electron-proton, proton-antiproton, proton-proton, and fixed target electron-nucleus data is used for the fits.

More than 5000 data points, and yet a $\chi^2/\text{dof} \approx 1$.

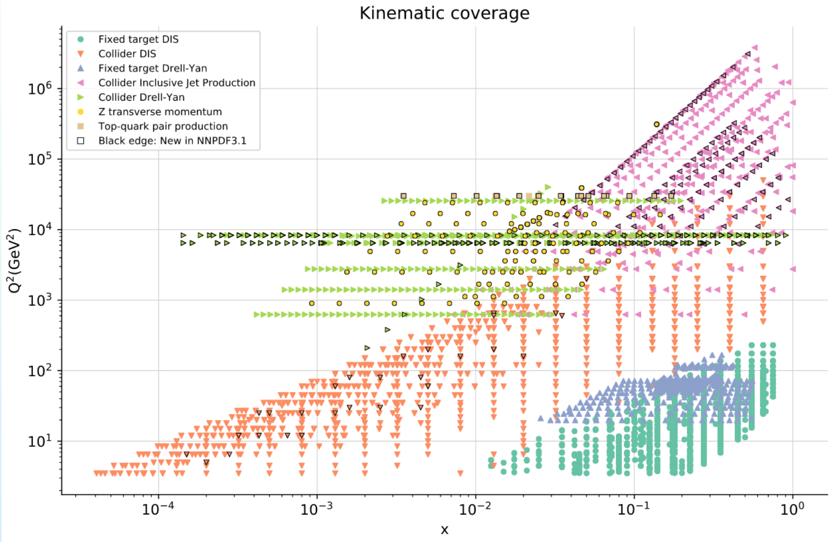

Strongest constraints on the proton structure come from HERA at DESY in Germany.
High-energy electron-proton collisions → probe deep inside the proton.

$E_e = 27.5$ GeV and $E_p = 920$ GeV $\rightarrow \sqrt{s} = 318$ GeV.

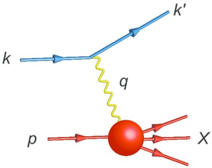

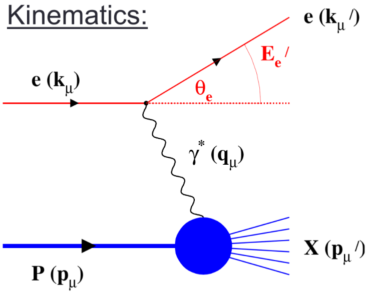

$s = 4\,E_t\,E_e$

$Q^2 = -q^2 = -(k_\mu - k'_\mu)^2$ — Measure of resolution power

$Q^2 = 2E_e E'_e(1 - \cos\Theta_{e'})$

$y = \frac{pq}{pk} = 1 - \frac{E'_e}{E_e}\cos^2\left(\frac{\theta'_e}{2}\right)$ — Measure of inelasticity

$x = \frac{Q^2}{2pq} = \frac{Q^2}{sy}$ — Measure of momentum fraction of struck quark

$$\frac{d^2\sigma}{dx dQ^2} = \frac{4\pi\alpha_{em}^2}{xQ^4}\left[\left(1 - y + \frac{y^2}{2}\right)F_2(x,Q^2) - \frac{y^2}{2}F_L(x,Q^2)\right] \quad (1)$$

$F_2(x,Q^2)$ is directly related to the parton densities in the proton. At zeroth-order in pQCD,

$$F_2(x,Q^2) \to F_2(x) = x\sum_f Q_f^2[q(x) + \bar{q}(x)]$$

$F_L(x,Q^2)$ is sensitive to the gluon densities. At LO, $F_L(x,Q^2) = 0$. $F_L(x,Q^2) \neq 0$ at $\mathcal{O}(\alpha_s)$.

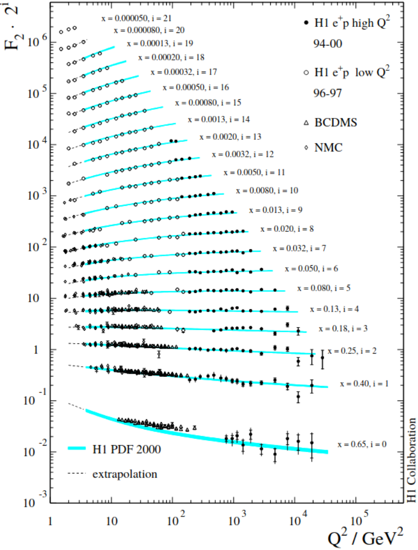

Evolution of $F_2(x, Q^2)$ correctly described by DGLAP, even outside its theoretical domain of application.

Historically, used to validate pQCD framework in extreme detail (*logarithmic* deviations!)

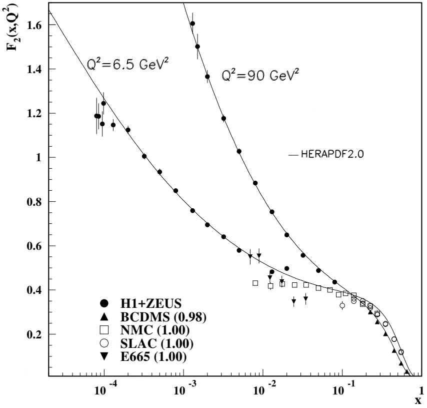

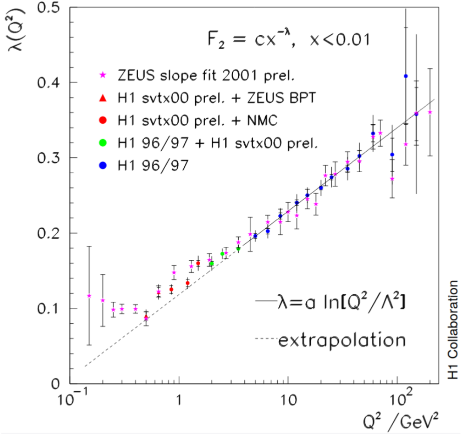

According to BFKL resummation, there should be a universal power-law growth of gluon densities at small-x,

$$xg(x, Q^2) \propto x^{-\lambda} \tag{2}$$

where $\lambda = \frac{N_c}{\pi} 4 \ln(2)\alpha_s \approx 0.5$. Growth is independent of Q^2 in BFKL.

This is contradiction with power-law fits to the data. Does this mean that BFKL is wrong?

Tension at small-x in global PDF fit analyses with DGLAP at NNLO

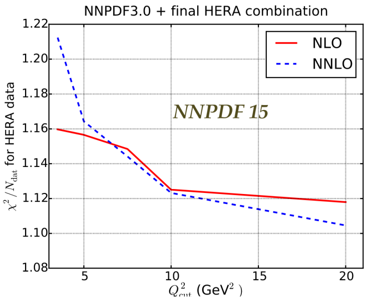

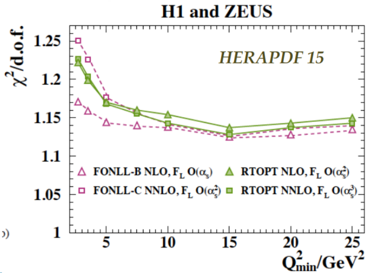

Global PDF fits with NNLO DGLAP evolution become unstable the more low Q^2 and low-x data is included in the analysis.

Possibly due to neglected BFKL resummation?

DGLAP at NNLO matched with BFKL resummation at small-x (NLLx)

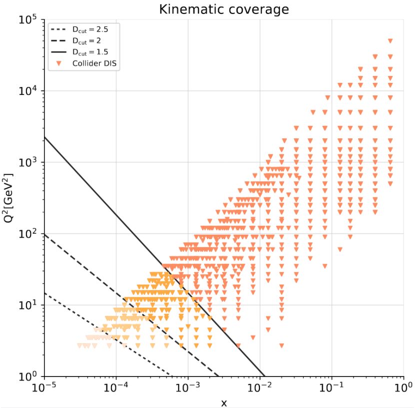

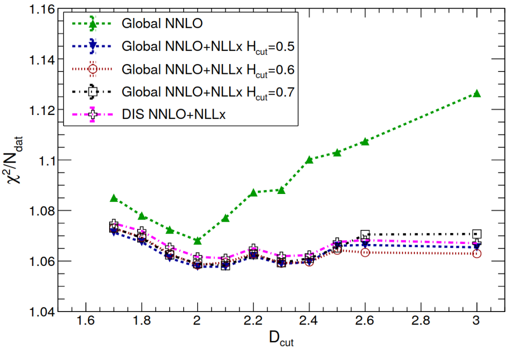

R. D. Ball, V. Bertone, M. Bonvini, S. Marzani, J. Rojo, L. Rottoli, Eur. Phys. J. C (2018) 78:321, arXiv:1710.05935

Recent NNPDF-like fit with NNLO DGLAP evolution matched to BFKL resummation at NLLx.

The more small-x data is included, the more stable the global fits become.

However, perturbativity can be questionnable for some of these data ($Q \gtrsim \Lambda_{QCD}$).

F_L is well-fit with NLLx resummation + NNLO DGLAP

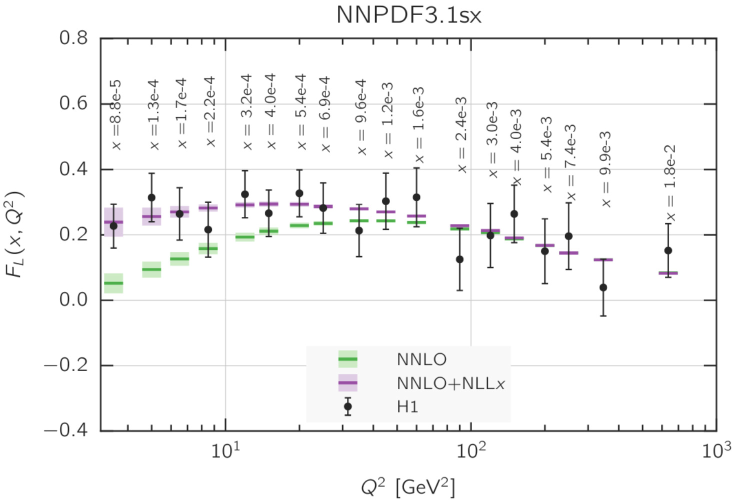

R. D. Ball, V. Bertone, M. Bonvini, S. Marzani, J. Rojo, L. Rottoli, Eur. Phys. J. C (2018) 78:321, arXiv:1710.05935

Most remarkably is the $F_L(x, Q^2)$ function fit at small-x → very sensitive to amount of glue in the proton.

Exclusive vector boson production ($\gamma^* p \to Vp$)

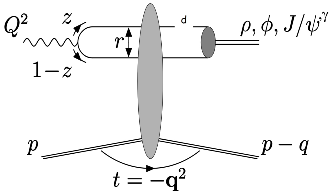

Quasi-real photon fluctuates into $q\bar{q}$, which as a color dipole that probes the proton structure.

Such interaction can lead to exclusive production of vector mesons ($V = \rho, \Upsilon, J/\psi$).

Process is very sensitive to gluon densities in the proton. At LO in pQCD,

$$\sigma_{\gamma^* p \to Vp} \propto [xg(x)]^2 \quad (3)$$

Small-x limit corresponds to large photon-proton masses, $W_{\gamma p}$.

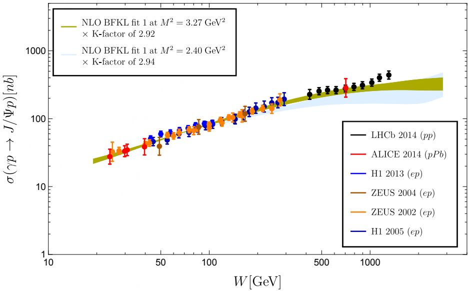

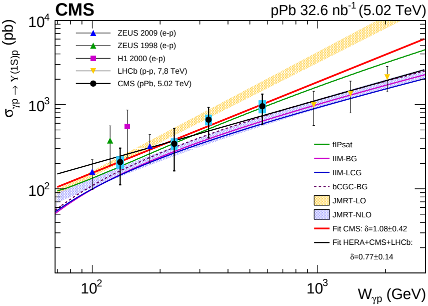

I. Bautista, A. Fernández-Téllez, M. Hentschinski, Phys. Rev. D 94, 054002, arXiv:1607.05203

CMS, Eur. Phys. J. C 79 (2019) 277 arXiv:1809.11080

Exclusive vector meson production in $\gamma^* p \to Vp$ scattering at high mass $W_{\gamma^* p}$. Predictions based on collinear PDFs give reasonable description of the data, as well as BFKL-based.

Incoming data from LHC experiments on exclusive J/ψ, $\psi(2s)$, Υ, ρ^0, ... at high $W_{\gamma^* p}$ will be crucial.

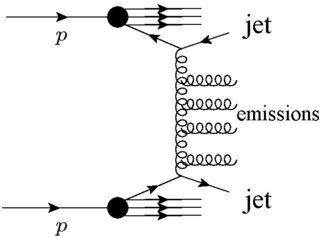

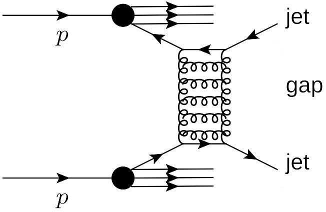

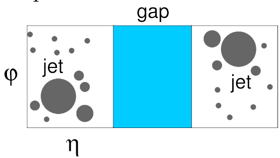

Mueller–Navelet jets:
Events where the two outermost jets are largely separated by a large interval in $\Delta y \equiv |y_{\text{jet1}} - y_{\text{jet2}}| \gg 1$.

At large Δy, the $\Delta\phi$ decorrelations between MN jets are stronger due to increased parton emission with the available phase-space.

$\Delta\phi$ decorrelations are expected to be strong in the BFKL picture.

Mueller–Tang jets:
Events with two jets separated by a rapidity gap (hard color-singlet exchange).

In $\Delta y \equiv |y_{\text{jet1}} - y_{\text{jet2}}| \gg 1$, it is expected to be described by perturbative pomeron exchange.

arXiv:1601.06713, JHEP08(2016)139

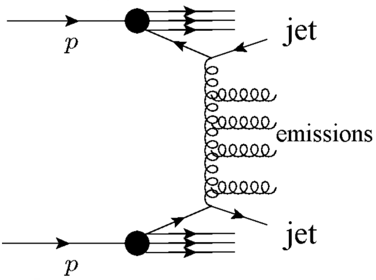

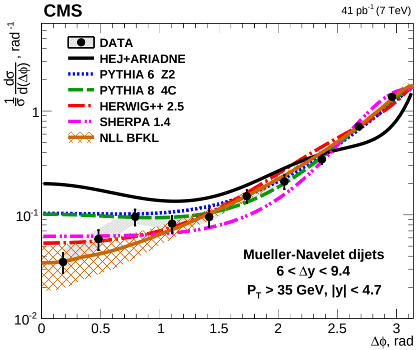

Analysis based on low pileup 7 TeV data. The Mueller–Navelet jets have $p_T > 35$ GeV and $|y| < 4.7$, anti-k_T jets with $R = 0.5$.

Characterize $\Delta\phi$ decorrelations as a function of $0 < \Delta y < 9.4$.

Average cosine of $\Delta\phi$ vs. $\Delta y \equiv |y_{\mathrm{jet1}} - y_{\mathrm{j2}}|$

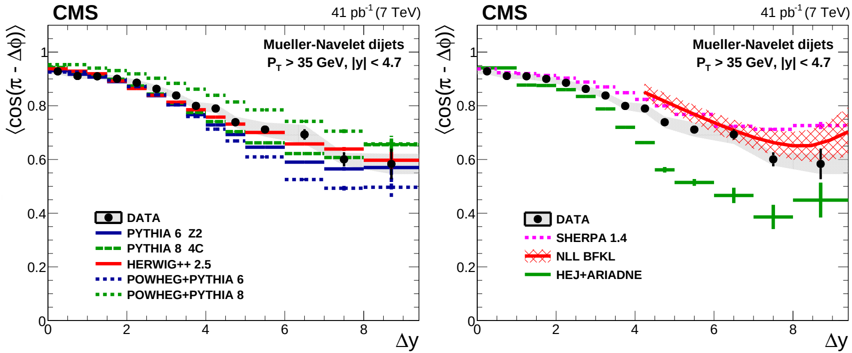

$$\cos(\pi - \Delta\phi) = 1 \iff \text{back-to-back jets}$$
$$\cos(\pi - \Delta\phi) = 0 \iff \text{collinear jets}$$

- BFKL at NLL + NLO impact factor calculations describe data at large Δy within uncertainties.
- PYTHIA6, PYTHIA8, HERWIG++ (DGLAP splitting functions) are able to describe data over wide range in Δy within uncertainties.
- POWHEG+PYTHIA6 and POWHEG+PYTHIA8 (NLO + PS) underestimates or overestimates data at large Δy, respectively.

Other $\langle \cos[n(\pi - \Delta\phi)] \rangle$ can be found in arXiv:1601.06713, JHEP08(2016)139.

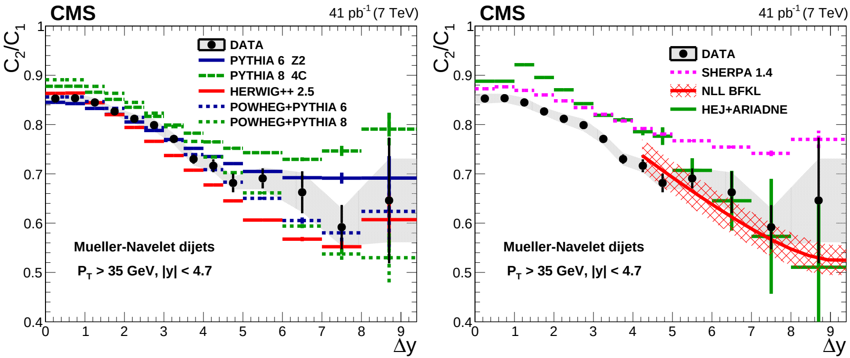

where $C_n \equiv \langle \cos[n(\pi - \Delta\phi)] \rangle$ is the n-th Fourier coefficient of the expansion of $\frac{1}{\sigma}\frac{d\sigma}{d(\Delta\phi)}$.

- BFKL at NLL + NLO impact factor calculations describe data at large Δy within uncertainties (B. Ducloué, L. Szymanowski, S. Wallon, JHEP 1305(2013) 096)
- SHERPA is not able to describe simultaneously the C_2/C_1 ratios and C_n coefficients versus Δy.
- PYTHIA6, POWHEG+PYTHIA6 are able to describe data over wide range in Δy within uncertainties.
- HERWIG++, PYTHIA8, POWHEG+PYTHIA8 slightly overshoot or undershoot data at large Δy, respectively.

Other ratio C_3/C_2 can be found in arXiv:1601.06713, JHEP08(2016)139.

- Difficult to clearly disentangle the onset of BFKL dynamics from other QCD perturbative and nonperturbative effects in Mueller–Navelet jets.
- A possibility for future measurements could be a combination of $\Delta\phi$ analysis and minijet-based observables (A. Sabio Vera, G. Chachamis, `BFKLex`, JHEP02 (2016) 064).

BFKL dynamics: looking for less inclusive variables

$$\langle p_T \rangle = \frac{1}{N} \sum_{i=1}^{N} |p_{Ti}|$$

$$\langle R_y \rangle = \frac{1}{N+1} \sum_{i=1}^{N+1} \frac{y_i}{y_{i-1}}$$

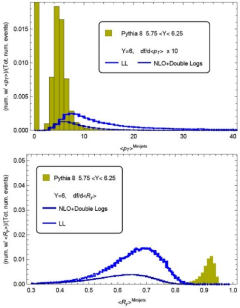

- Looking for multiple gluon emission along ladder characteristic of BFKL: number, p_T, rapidity distributions of "minijets"
- Comparison between BFKL-ex MC and pythia/herwig to find best variables: collaboration with A. Sabio Vera, D, Gordo, G. Chachamis, F. Deganutti, T. Raben

slide by C. Royon

CMS-TOTEM Collaborations, arXiv:2102.06945, *accepted by PRD*

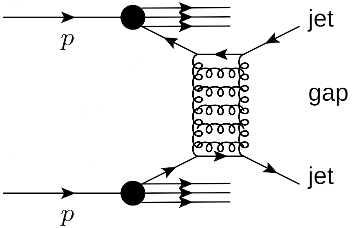

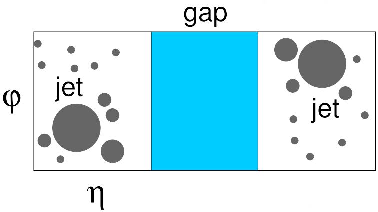

t-channel color-singlet exchange between partons (two-gluon exchange)
$\rightarrow$ η **interval void of particles between jets (pseudorapidity gap)**.

In the high-energy limit, this corresponds to **perturbative pomeron exchange** (BFKL two-gluon ladder exchange).

DGLAP dynamics are strongly suppressed in events with pseudorapidity gaps (Sudakov form factor to suppress radiation in gap).

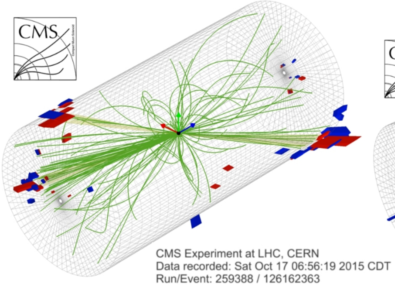

Color-exchange event candidate
(Background-like)

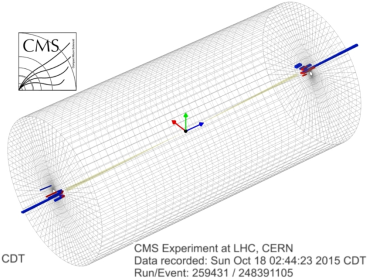

Color-singlet exchange event candidate
(Signal-like)

Leading two jets $p_T > 40$ GeV, all other jets $p_T > 15$ GeV, calorimeter towers with $E > 1$ GeV, charged particles with $p_T > 200$ MeV

Analysis based on low-pileup data. Event selection:

- Particle-flow, anti-k_t jets $R = 0.4$.
- Two highest p_T jets have $p_T > 40$ GeV each.
- Leading two jets satisfy $1.4 < |\eta_{\rm jet}| < 4.7$ and $\eta^{\rm jet1}\eta^{\rm jet2} < 0$
  $\rightarrow$ **Favors t-channel color-singlet exchange.**

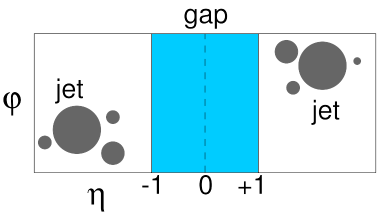

Pseudorapidity gap is defined by means of the charged particle multiplicity N_{tracks} between the leading two jets. Each charged particle has $p_T > 200$ MeV in $|\eta| < 1$.

Results on color-singlet exchange fraction f_{CSE}

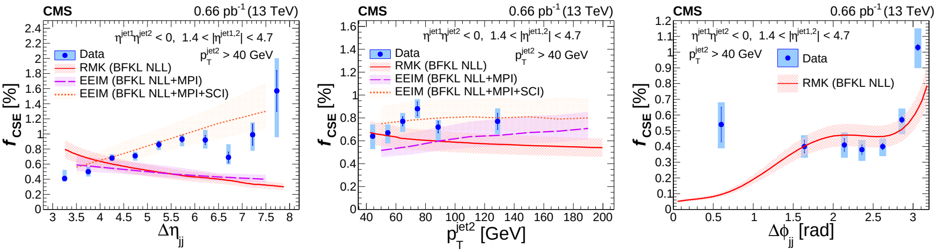

- **Color-singlet exchange represents ≈ 0.6% of the inclusive dijet cross section for the probed phase-space.**
- Bars represent stat uncertainties, boxes represent stat + syst uncertainties.
- Comparison w/ calculations based on BFKL NLL resummation + LO impact factors:
  - **Royon, Marquet, Kepka** (**RMK**) predictions (Phys. Rev. D 83.034036 (2011), arXiv:1012.3849), with survival probability $|S|^2 = 0.1$.
  - **Ekstedt, Enberg, Ingelman, Motyka** (**EEIM**) predictions (Phys. Lett. B 524:273 and arXiv:1703.10919) with MPI to simulate $|S|^2$, also be supplemented with soft-color interactions (SCI).
- **Challenging to describe theoretically all aspects of the measurement simultaneously.**
- Higher-order corrections are being prepared.

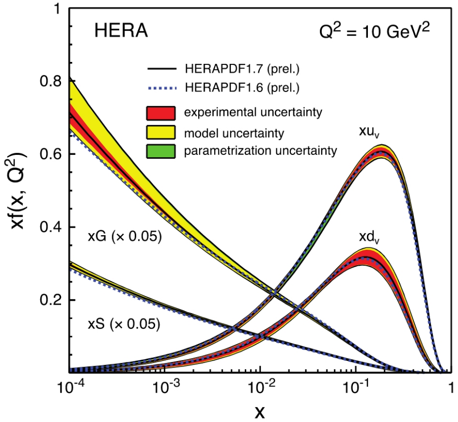

gluon emission

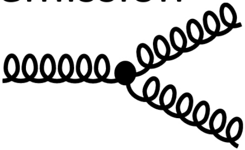

BFKL/DGLAP evolution includes only parton splitting. The parton densities should increase indefinitely.

Serious problem: **violation of unitarity!** Hadronic cross sections and the proton and nuclei are finite. Is QCD jeopardized?

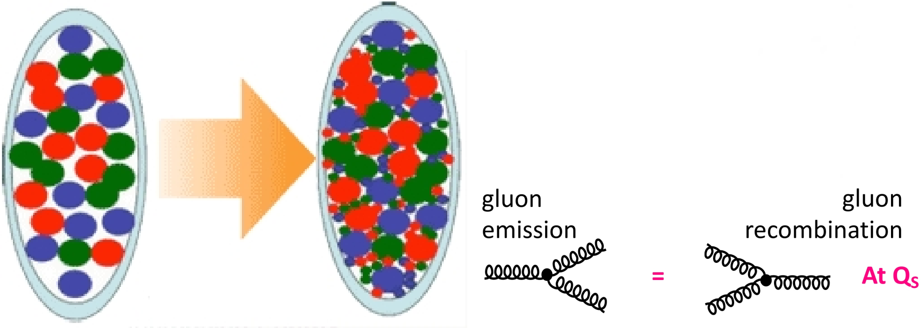

The occupancy of gluons inside the proton becomes so large that, at some point, recombination effects take place.

Parton saturation occurs when the splitting and recombination mechanisms balance each other.

This occurs at a special energy scale known as the saturation scale, $Q_s^2(x) \propto 1/x^{\lambda}$, where $\lambda \approx 0.3$. Theoretically described by Balitsky–Kovchegov (BK) equation.

Gluon densities with gluon splitting and recombination

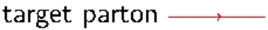

Gluon densities with gluon splitting and recombination

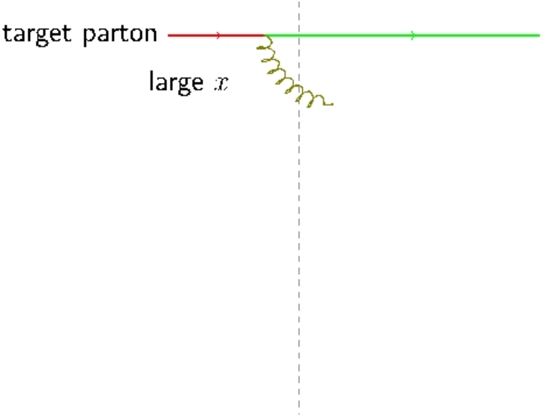

Gluon densities with gluon splitting and recombination

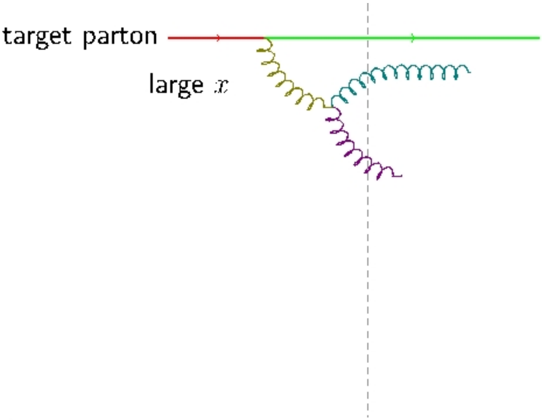

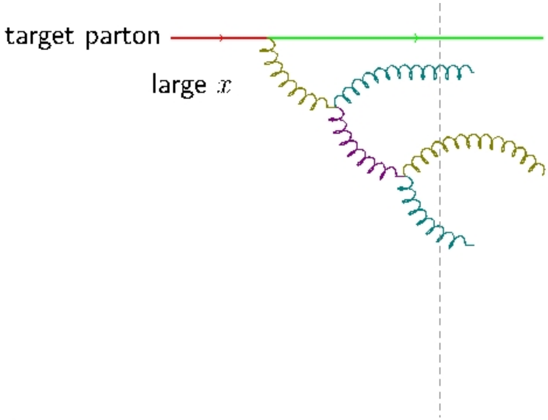
target parton
large x

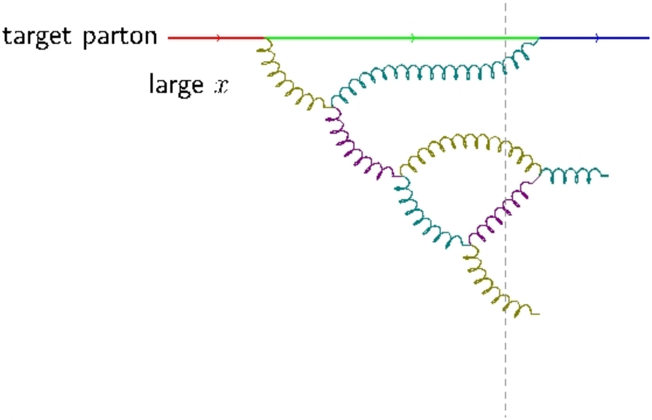
target parton
large x

Gluon densities with gluon splitting and recombination

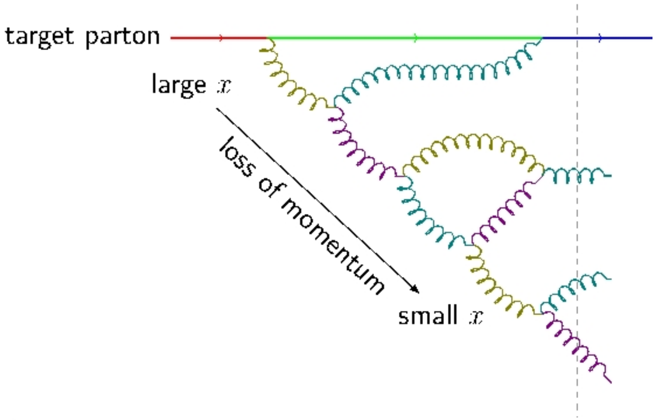

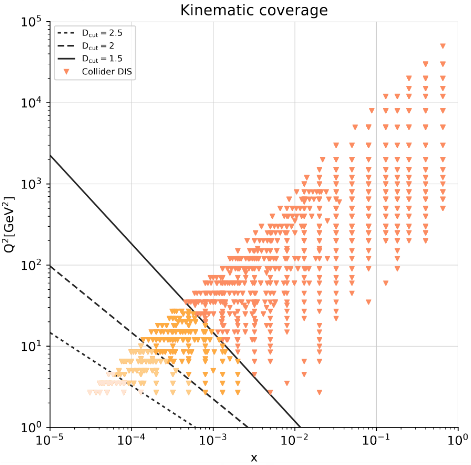

The onset of saturation is expected to occur at $Q_s^2 \approx 7$ GeV^2 at $x = 10^{-5}$.

No data in this region! Constrained by $\sqrt{s} = \sqrt{Q_s^2/x}$

We would need $\sqrt{s} \approx 1$ TeV electron-proton collisions. **Very expensive to have such setup.**

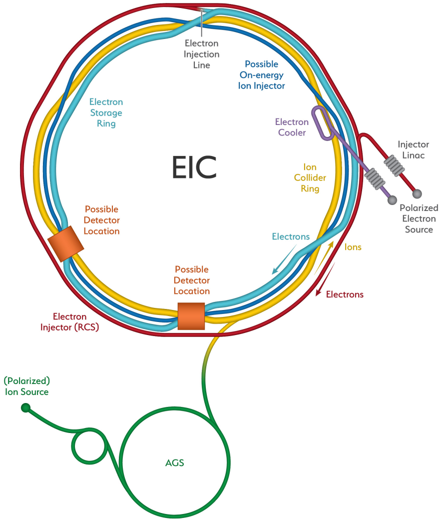

3.9 km of circumference electron-ion collider. **Perform DIS in the first electron-nucleus collider.**

Use existing Relativistic Heavy Ion Collider (RHIC) facility at BNL for ion beams + electron beam (polarized or unpolarized).

$\sqrt{s} = 20$ and up to 140 GeV. Various ion species with a range of beam energies (Ca, Au).

Several “blessings” by U.S. bodies (National Academy of Sciences, Department of Energy CD-1 approval, ...).

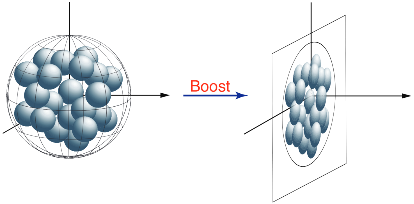

Q_s^2 is expected to scale with $A^{1/3}$, where A is the number of nucleons of the ion,

$$Q_s^2 \propto (A/x)^{1/3}$$

For a gold nucleus (Au), we can probe parton saturation at $Q_s^2 = 7$ GeV^2 for moderate $x = 10^{-3}$.

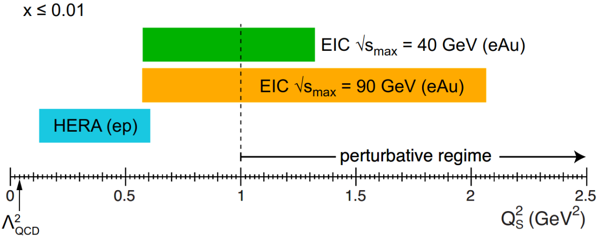

Projections with pseudodata

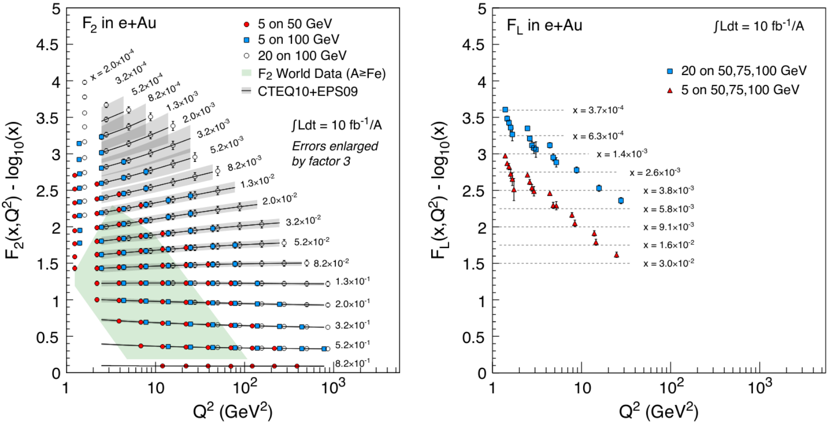

EIC White Paper, arXiv:1212.1701

- 3D picture of the proton: transverse momentum k_T, impact parameter b, x.

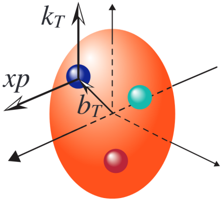

- Addressing the proton spin puzzle.

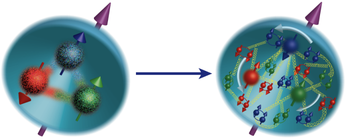

- Interaction of partons and hadrons with cold QCD matter.

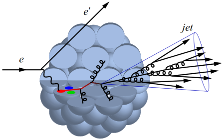

- QCD is a extremely rich and complex theory that keeps delivering many exciting surprises.
- The dynamics of multiple gluon splittings has yet to be understood experimentally and theoretically.
- Plenty of work to do with LHC data, in preparation for the future EIC.

Thanks!

DE-SC0019389

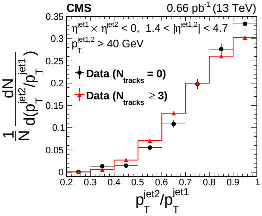

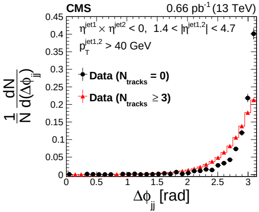

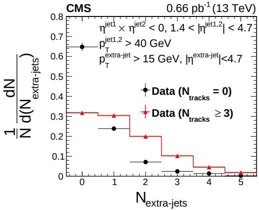

Normalized distributions in:

- $p_T^{\text{jet2}} / p_T^{\text{jet1}}$.
- $\Delta\phi_{jj} = |\phi^{\text{jet1}} - \phi^{\text{jet2}}|$
- Jet multiplicity $N_{\text{extra-jets}}$ for jets with $p_{T,\text{extra-jet}} > 15$ GeV.

Jet-gap-jet candidates with $N_{\text{tracks}} = 0$ and events dominated by color-exchange dijet events with $N_{\text{tracks}} \geq 3$.

Distributions reflect underlying quasielastic parton-parton scattering process topology.

Turning to study with intact protons (CMS-TOTEM)

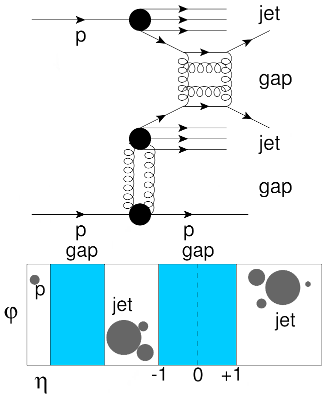

Better understand the role of spectator partons in the destruction of the central gap.

Same dijet and central gap definitions as with CMS-only analysis.

Proton requirements:

- The fraction of beam energy lost by the proton must be $\xi_p(\text{RP}) < 0.2$
- The four-momentum transfer square at the proton vertex must be $-4 < t < -0.025$ GeV^2, where $t = (p_f - p_i)^2$ of the proton.

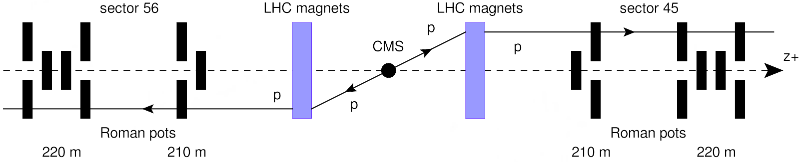

Results on p-gap-jet-gap-jet

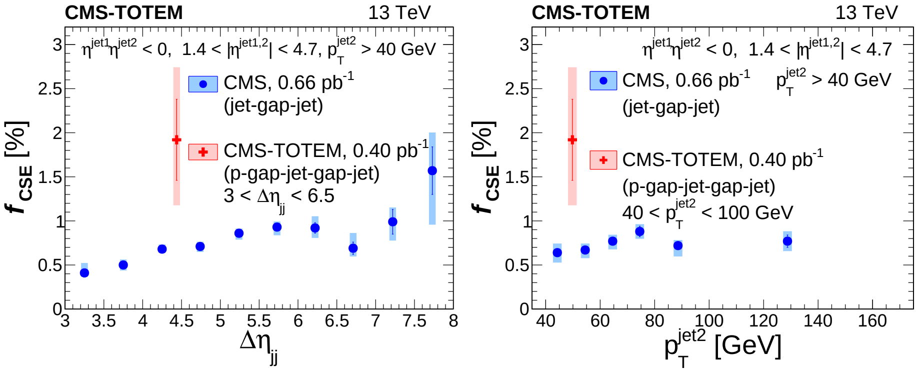

f_{CSE} fraction in p-gap-jet-gap-jet study is $2.91 \pm 0.70(\mathrm{stat})^{+1.02}_{-0.94}(\mathrm{syst})$ times larger than jet-gap-jet fraction, for similar dijet kinematics.

Abundance of events with a central gap is larger in events with intact protons.

Demonstrated feasibility for more detailed studies with future data.

Consistent with other two-rapidity gap topology

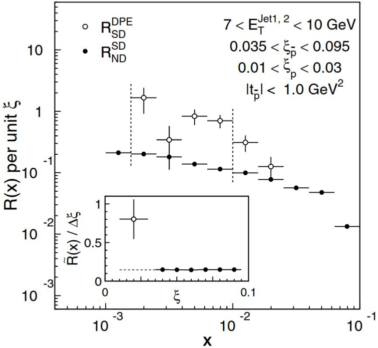

CDF studied double-pomeron exchange/single-diffractive dijet event ratios, compared them to single-diffractive/non-diffractive (**PRL85,4215**):

$\mathcal{R}$ = (DPE/SD) / (SD/ND) $= 5.3 \pm 1.9$, different from factor of 1 expected from factorization. Comparison of gap-jet-jet-gap/gap-jet-jet topology.

Present CMS-TOTEM result finds a similar effect for a different two-gap topology (proton-gap-jet-gap-jet).

Systematic uncertainty table summary

Source	Jet-gap-jet $\Delta\eta_{jj}$	Jet-gap-jet $p_{T,\,jet-2}$	Jet-gap-jet $\Delta\phi_{jj}$	Proton-gap-jet-gap-jet
Jet energy scale	1.0–5.0	1.5–6.0	0.5–3.0	0.7
Track quality criteria	6.0–8.0	5.4–8.0	1.5–8.0	8
Charged particle p_T threshold	2.0–5.8	1.6–4.0	1.1–5.8	11
Background subtraction method	4.7–14.6	2–14.6	12.0	28.3
NBD fit parameter	0.8–2.6	0.6–1.7	0.1–0.6	7
NBD fit interval	—	—	—	12.0
Calorimeter energy scale	—	—	—	5.0
Horizontal dispersion	—	—	—	6.0
Fiducial selection requirements	—	—	—	2.6
Total	6.8–22.0	8.3–14.9	12.0–17.1	33.4

Relative systematic uncertainties in percentage on f_{CSE}. Uncertainty range is representative of the variation found in the jet-gap-jet fraction in bins of the kinematic variables of interest.

Proton selection

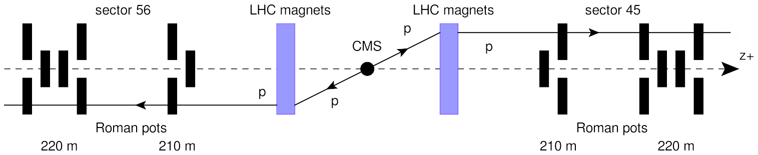

- At least one proton on either side.
- Track-impact point cuts (x, y) based on acceptance studies. For vertical RPs, $0 < x < 20$mm and $8 < |y| < 30$mm, for horizontal RPs, $7 < x < 25$mm and $|y| < 25$mm.
- Proton fractional momentum loss is $\xi_p(\text{RP}) < 0.2$ and four-momentum transfer square is $0.025 < -t < 4$ GeV^2. Based on acceptance studies + validity of optical functions.
- To suppress beam bkg contribution (pileup+beam halo), additional cut $\xi_p(\text{PF}) - \xi_p(\text{RP}) < 0$, where $\xi_p(\text{PF}) = \frac{\sum_i E_i \pm p_{z,i}}{\sqrt{s}}$ is the proton fractional momentum loss reconstructed with PF candidates of CMS. The $\pm$ is the sign of the intact proton η.

A total of 336 and 341 events in sector 45 and sector 56, respectively, satisfy the above selection requirements + dijet selection requirements.

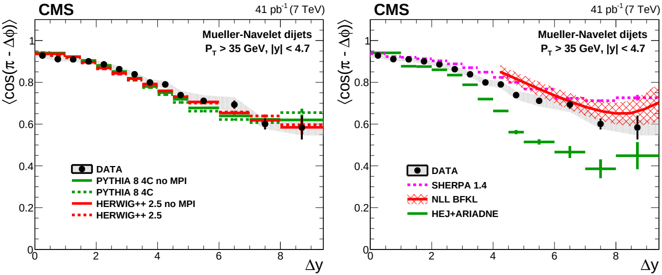

CMS, JHEP 08 (2016) 139, arXiv:1601.06713

Some standard probes of BFKL dynamics:

- $\Delta\phi$ decorrelations in Mueller–Navelet jets (Plot above)
- Exclusive vector meson production ($\gamma^* p \to Vp$) at large $W_{\gamma p}$, with $V = J/\psi, \psi(2s), \Upsilon, \ldots$.
- PDFs at small-x_{Bj} at small momentum transfer $Q^2 > \Lambda^2_{QCD}$.

It is generally difficult to isolate BFKL from other higher-order effects, such as DGLAP evolution. Processes where DGLAP evolution is expected to be suppressed may aid to unambiguously identify BFKL dynamics.

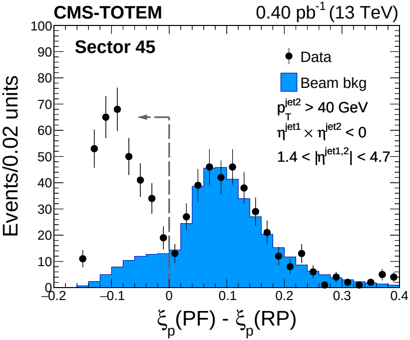

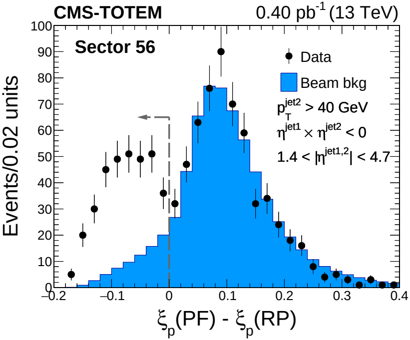

Estimated with event-mixing: inclusive dijet events paired with protons in zero-bias sample.

Requirement $\xi_p(\mathrm{PF}) - \xi_p(\mathrm{RP}) < 0$ indicated by dashed line. Region $\xi_p(\mathrm{PF}) - \xi_p(\mathrm{RP}) > 0$ is dominated by beam bkg contributions → Used as control region to estimate residual beam bkg in $\xi_p(\mathrm{PF}) - \xi_p(\mathrm{RP}) < 0$.

Beam background contributes 18.7 and 21.5% for protons in sector 45 and 56 in $\xi_p(\mathrm{PF}) - \xi_p(\mathrm{RP}) < 0$, respectively.

Inclusive dijet production + uncorrelated proton from residual pileup or beam halo activity (estimade from data).
Standard diffractive dijet production with no central gap (p-gap-jet-jet topology):

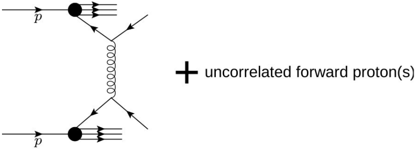

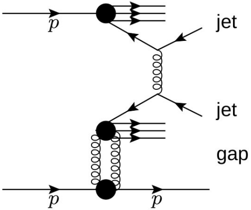

→ Fluctuations on particle multiplicity can lead to gaps. Needs to be subtracted (NBD and ES methods).

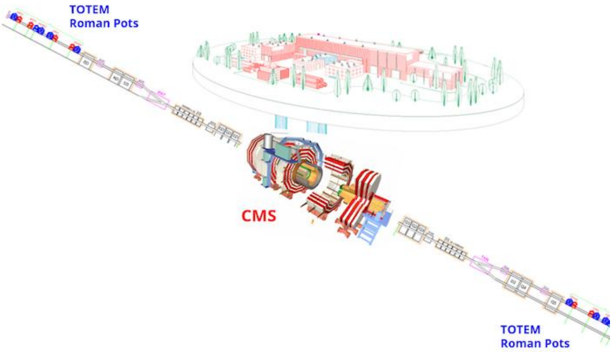

CMS:

- General purpose detector at IP5 of the CERN LHC.
- Tracking ($|\eta| < 2.5$), and hadronic and electromagnetic calorimetry ($|\eta| < 5.2$)
- Jets reconstructed within $|\eta^{\text{jet}}| < 4.7$.

TOTEM:

- **Roman pots:** Forward tracking detectors at $\approx$ 220m w.r.t. IP5 that measure the protons scattered at small angles w.r.t. the beam.
- Measurement of total cross section, elastic scattering, and soft and hard diffractive processes in pp collisions.

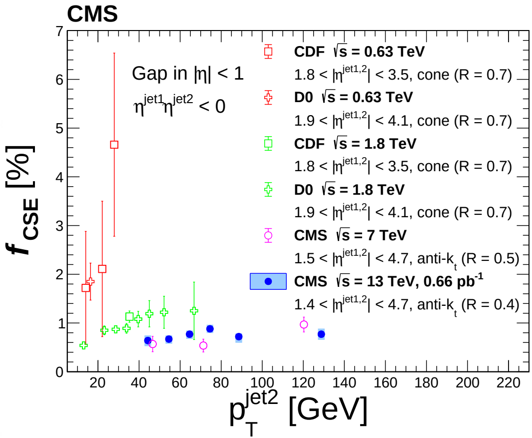

- Measurement of jet-gap-jet events at four different $\sqrt{s}$ in $p\bar{p}$ and pp collisions at 0.63 TeV, 1.8 TeV, 7 TeV, and 13 TeV (this measurement).
- Generally, f_{CSE} is expected to decrease with increasing $\sqrt{s}$, due to an increase in spectator parton activity with $\sqrt{s}$.
- Within uncertainties, f_{CSE} stop decreasing with $\sqrt{s}$ at LHC energies, in contrast to trend observed at lower energies 0.63 TeV → 1.8 TeV → 7 TeV.

f_{CSE} vs. $\Delta\eta_{jj}$ between 7 and 13 TeV CMS results

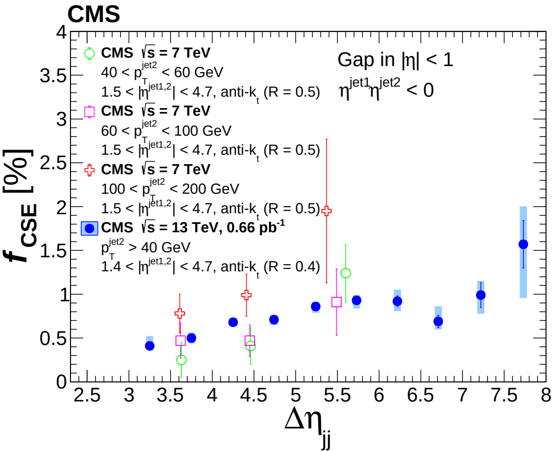

- CMS 7 TeV analysis performed in three bins of p_T^{jet2} and three bins of $\Delta\eta_{jj} = 3$–4, 4–5,5–7 (CMS, **EPJC** 78 (2018) 242)
- **Trend of increasing f_{CSE} with $\Delta\eta_{jj}$ is confirmed with new 13 TeV results.**
- **New results reach previously unexplored values of $\Delta\eta_{jj}$**

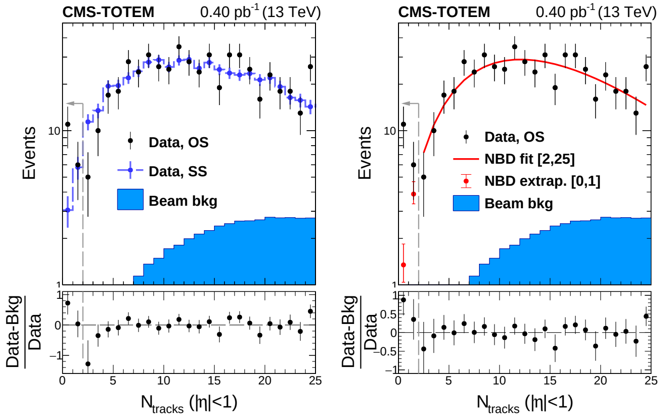

Similar techniques to estimate background from fluctuations in N_{tracks}:

- Control dijet sample: Two jets in same side w.r.t. fixed η region. η interval is be adjusted to account for SD dijets boosts.
- Negative binomial distribution (NBD) approach: NBD is fit in $2 < N_{\text{tracks}} < 25$, and extrapolated down to $N_{\text{tracks}} = 0$.

Excess of events at low N_{tracks} → For the first time these events are studied!

Filled histogram represents beam background contribution.

Soft-parton activity can destroy the central gap between the jets. This is parametrized with a gap survival probability, $|\mathcal{S}|^2$, **which is difficult to understand theoretically.**

In pp collisions with intact protons, soft-parton activity is largely suppressed → **Central gap more likely to "survive"** (Marquet, Royon, Trzebiński, Žlebčík, Phys.Rev. D 87, 034010 (2013)).

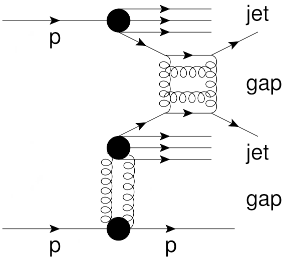

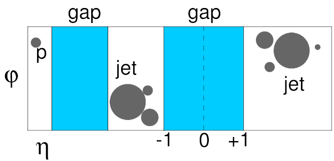

Addressed in study with CMS-TOTEM combined analysis (arXiv:2102.06945). **Second part of the analysis**.

Color-exchange
(single-gluon in
t-channel)

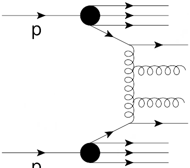

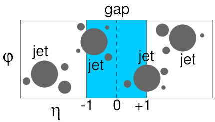

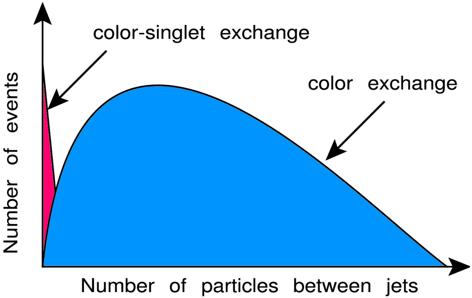

Color-singlet exchange
(two-gluon in t-channel)

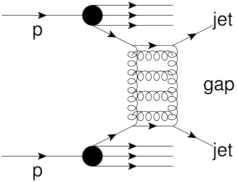

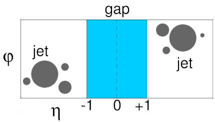

Color-exchange fluctuations at low-multiplicities need to be properly treated.

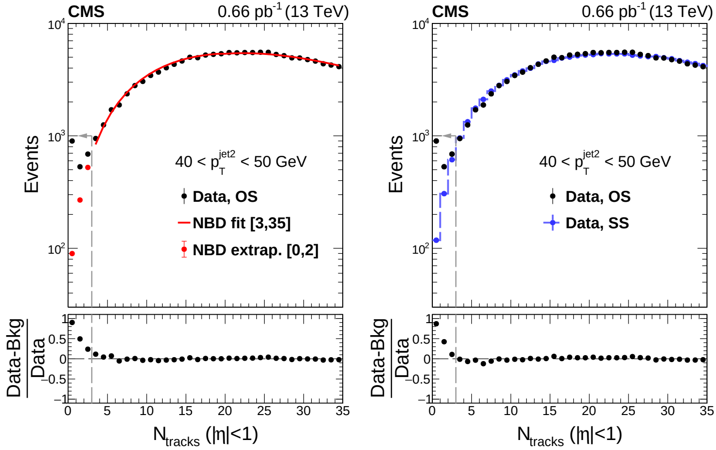

Color-exchange events dominate at large N_{tracks} $\rightarrow$ Use as control region to estimate fluctuations at low N_{tracks}. Two data-based approaches:

- Control dijet sample: two jets on the same-side (SS) of the CMS detector, $\eta^{\text{jet1}}\eta^{\text{jet2}} > 0$. Normalize to events with jets in opposite sides (OS) of CMS, $\eta^{\text{jet1}}\eta^{\text{jet2}} < 0$, in $N_{\text{tracks}} > 3$.
- Negative binomial distribution (NBD) function: Fit data with NBD in $3 \leq N_{\text{tracks}} \leq 35$, extrapolate down to $N_{\text{tracks}} = 0$. (Baseline method)

Hard color-singlet exchange fraction f_{CSE}

We extract the fraction f_{CSE} based on the charged particle multiplicity between the jets:

$$f_{\text{CSE}} \equiv \frac{N(N_{\text{tracks}} < 3) - N_{\text{bkg}}(N_{\text{tracks}} < 3)}{N_{\text{all}}} \equiv \frac{\text{color-singlet exchange dijet events}}{\text{all dijet events}}$$

The fraction f_{CSE} is measured as a function of:

- $\Delta\eta_{\text{jj}} \equiv |\eta^{\text{jet1}} - \eta^{\text{jet2}}|$: Sensitive to expected BFKL dynamics, since it's related to resummation of large logs of s.
- $p_{\text{T}}^{\text{jet2}}$: Sensitive to expected BFKL dynamics; allows for comparison at lower $\sqrt{s}$.
- $\Delta\phi_{\text{jj}} \equiv |\phi^{\text{jet1}} - \phi^{\text{jet2}}|$: Sensitive to deviations of $2 \to 2$ scattering topology of color-singlet exchange.

- B.S. in Physics at Universidad de Sonora in Mexico.

- Ph.D. in Physics at the University of Kansas with Prof. Christophe Royon
  - Jet measurements with CMS and TOTEM experiments.
  - Particle physics phenomenology (photon-photon physics).

- Next step: Postdoctoral position at the École Polytechnique in France.
- Research in heavy-ion physics with CMS experiment.